Revealing subsalt structure using RTM 3D dip gathers

Yi Huang[1], Yang Li[1], Chang-Chun Lee[1], Sabaresan Mothi[1], and Yan Huang[1]

Abstract

Gulf of Mexico (GoM) subsalt imaging often suffers from poor illumination due to salt-related wavefield distortion, even with full-azimuth (FAZ) acquisition. In order to image the weakly illuminated subsalt plays, isolating the signal from the noise is a crucial component of many depth-imaging practices. Reverse time migration (RTM) subsurface 3D dip-azimuth gathers, which separate seismic data into different dip/azimuth components, are utilized to address illumination problems in structure-oriented imaging. A weighting scheme using RTM 3D dip gathers for image enhancement is proposed; it is based on a priori structure information and targets noise that has conflicting dips with the structure. The sensitivity of the method to the uncertainty of the initial dipping information of the structure is further discussed and evaluated. The method is applied on subsalt structures on both a synthetic data set and a real data set with staggered-acquisition FAZ data. The tests demonstrate the necessity of signal-to-noise ratio enhancement in the imaging of FAZ, long-offset data, and the effectiveness of RTM 3D dip gathers in unmasking poorly illuminated zones.

Introduction

Imaging subsalt reflections often requires illumination from several azimuths or undershooting of complex salt bodies via long-offset acquisitions. Driven by the imaging challenges of deepwater subsalt plays, FAZ and long-offset acquisitions have been embraced rapidly by the oil and gas industry because of their ability to provide information about geologic features that otherwise may be unresolvable with more limited surface data. Despite the upgrade in acquisition technologies, areas of weak illumination still exist due to complex geology, and in these areas only a limited amount of energy may be reflected back to be recorded at the surface. Besides poor illumination, coherent noise such as mode-converted waves (Huang et al., 2013), residual noise, and residual multiples can generate migration artifacts, which in extreme cases can overwhelm even the true events. Strengthening illumination or increasing the signal-to-noise ratio (S/N) of the data is often required.

Least-squares migration (LSM) (Nemeth et al., 1999) was proposed to solve imaging problems associated with poor illumination issues. An optimized image and reflectivity model can be achieved by minimizing the mismatch between demigrated and acquired seismic data, intrinsically healing illumination issues through the inversion process. Unfortunately, the reliability of the demigration (because of modeling limitations and inaccurate velocity models) and the high computational cost (especially with high frequencies) are both major challenges for practical implementations of LSM.

The demand for improving the S/N of subsalt targets has led in practice to the emergence of a variety of more practical illumination-compensation techniques, some of which can be considered as simplified versions of LSM. These techniques normally use an existing approximate velocity model and/or interpreted subsurface target reflectors to separate signal from noise through a modeling/demigration process.

The illumination-based weighting of RTM angle gathers (Gherasim et al., 2010) is one such S/N-enhancement approach that uses both a priori models and structure information. It uses the wave equation to model illumination as a function of opening angle and compensates the illumination in the subsurface opening angle/azimuth domain in order to improve the amplitude-versus-angle (AVA) response. A major drawback is that any updates to interpretations of target reflectors or subsalt velocities require repetitive analyses, which can drive up the cost if multiple iterations are required.

Point-spread function (PSF) based illumination-compensation and amplitude-inversion approaches do not require interpretation of subsalt reflectors. The various illumination effects associated with the acquisition and an initial velocity model are simulated by the demigration-remigration of point diffractors (Fletcher et al., 2012). The "eyeball" illumination approach suggested by Ting et al. (2010) shares a concept very similar to PSF. The advantage of PSF-related techniques is that they are free of subsalt assumptions, but this also limits their capacity to be used for signal and noise separation. In regions of extremely poor illumination, where coherent noise and migration artifacts can dominate signal, the S/N rebalancing across spatial locations and dip orientations may not be sufficient. Also, the cost is still significant for precisely modeling the wave propagation through finite-difference (FD) modeling. Salt boundaries may lead to problems, even for full-wave PSFs, because of stark velocity contrasts. Ray tracing-based approaches, though less expensive, may suffer even more.

To fully enhance the signal passing through poorly illuminated areas without boosting the weak noise, vector offset output (VOO) RTM (Q. Xu et al., 2011) combined with a modified deconvolution imaging condition (Chazalnoel et al., 2012) is used frequently in GoM imaging. Though we list only two references for discussion here, similar techniques have been used to improve the subsalt image. The idea of these techniques is to separate energy into different image partitions that correspond to different dip directions after the imaging condition. Coherent noise often can be differentiated from the signal and attenuated, purely using a priori knowledge of the subsurface structure to scale the partitions before stacking. In some cases, subjective interpretations are used to generate the a priori information, which can bring uncertainty to the results.

To minimize the uncertainty, various experiments with different interpretation scenarios can be implemented. Since they use only postmigration energy partitions, the overall cost is still low, even for several scenarios. In general, dips are well separated using VOO RTM; however, conflicting dips may still exist in a single VOO partition. This is because the separation is based on the relative offset of the source and imaging location, which is only indirectly related to the dip of the subsurface events.

Li et al. (2012) proposed a PSF-like approach for evaluating and balancing dip- and azimuth-dependent illumination coverage through forward modeling point diffractors followed by RTM with 3D subsurface dip-azimuth gather outputs. Subsurface dip-azimuth

[1]CGG.

http://dx.doi.org/10.1190/tle35030228.1.

RTM gathers (hereafter referred to as RTM 3D dip gathers or simply dip gathers) can accurately map the prestack depth-migration image into different subsurface dip orientations using plane-wave decomposition applied during the imaging condition.

We propose an interpretation-aided weighting technique to be applied to the RTM 3D dip gathers for S/N enhancement by taking advantage of the accuracy of both the signal splitting in dip gathers and the idea of weighting partitions used in VOO RTM. No additional FD modeling is required to evaluate different interpretation scenarios in this method. To address the concerns on the impact of interpretation uncertainties for subsalt image enhancement, we perform a sensitivity analysis on different interpretation scenarios using a modified version of the SEAM model. We also apply this method to FAZ data acquired with a staggered acquisition (Mandroux et al., 2013) in the GoM to demonstrate its effectiveness and importance for imaging data acquired by recent rich-azimuth acquisition configurations.

RTM dip gathers

S. Xu et al. (2011) described the formulation of RTM 3D angle gathers for common shot migration with a crosscorrelation imaging condition. The general idea involves performing a 4D temporal/spatial Fourier transform to obtain the source and receiver wavefields in the frequency/wavenumber domain, computing the phase direction of the wave propagation from the spatial wavenumber vectors, and decomposing the image by subsurface reflector incident and azimuth angles (θ_i, ϕ_i).

In general, the RTM-migrated image can be decomposed based on four subsurface angles, namely the incidence-azimuth angles at the reflector (θ_i, ϕ_i) and the dip-azimuth angles (θ_d,ϕ_d); they are denoted by $I(\vec{\boldsymbol{k}},\theta_d,\phi_d,\theta_i,\phi_i)$ in the frequency/wavenumber domain (equations 1 and 2).

$$I(\vec{\boldsymbol{k}},\theta_d,\phi_d,\theta_i,\phi_i) = \sum_{\omega}\sum_{(\boldsymbol{k}_r-\boldsymbol{k}_s)}\delta(\theta-\theta_d)\delta(\phi-\phi_d)\delta(\theta-\theta_i)\delta(\phi-\phi_i)\times p_F(\boldsymbol{k}_s,\omega)\,p_B(\boldsymbol{k}_r,\omega), \quad (1)$$

and

$$\begin{aligned}
\cos(\theta_i) &= \frac{(\boldsymbol{k}_s+\boldsymbol{k}_r)\cdot\boldsymbol{k}_r}{|\boldsymbol{k}_s+\boldsymbol{k}_r||\boldsymbol{k}_r|},\\
\cos(\phi_i) &= \frac{(\boldsymbol{k}_s\times\boldsymbol{k}_r)\cdot(\boldsymbol{n}_x\times(\boldsymbol{k}_s+\boldsymbol{k}_r))}{|\boldsymbol{k}_s\times\boldsymbol{k}_r||\boldsymbol{n}_x\times(\boldsymbol{k}_s+\boldsymbol{k}_r)|},\\
\cos(\theta_d) &= \frac{(\boldsymbol{k}_s+\boldsymbol{k}_r)\cdot\boldsymbol{n}_z}{|\boldsymbol{k}_s+\boldsymbol{k}_r|},\\
\cos(\phi_d) &= \frac{\boldsymbol{n}_x\cdot(\boldsymbol{n}_z\times((\boldsymbol{k}_s+\boldsymbol{k}_r)\times\boldsymbol{n}_z))}{|(\boldsymbol{n}_z\times((\boldsymbol{k}_s+\boldsymbol{k}_r)\times\boldsymbol{n}_z)|}.
\end{aligned} \quad (2)$$

Here, n_x is the unit vector along the x coordinate; the wavenumber vectors $\boldsymbol{k}_s$ and $\boldsymbol{k}_r$ are the wave propagation phase directions at the subsurface reflection point for the wavefields from the source location and the receiver location, respectively. p_F and p_B are the corresponding forward/source and backward/receiver wavefields. Figure 1 illustrates the incident-azimuth and dip-azimuth angle definition in RTM 3D dip angle gathers at a subsurface reflector. The grey surface in Figure 1 represents a subsurface reflector, and $\boldsymbol{k}$ is the vector sum of $\boldsymbol{k}_s$ and $\boldsymbol{k}_r$.

The inverse Fourier transform of the quantity in equation 1 is the desired 3D migrated image indexed by incidence and dip angles, which occupies a seven-dimensional space. This is a big challenge in terms of data storage. To keep data size manageable, we generated two different RTM gathers: one by incidence angle decomposition (incidence angle gather), $IAG(\vec{x},\theta_i,\phi_i)=\Sigma_{(\theta_d,\phi_d)}I(\vec{x},\theta_d,\phi_d,\theta_i,\phi_i)$, and the other by dip angle decomposition (dip angle gather), $DAG(\vec{x},\theta_d,\phi_d)=\Sigma_{(\theta_i,\phi_i)}I(\vec{x},\theta_d,\phi_d,\theta_i,\phi_i)$. The former are typically used to measure velocity errors; the latter are used to improve image response. Figure 2 illustrates the different appearance of an RTM 3D (incidence) angle gather and a dip gather generated from a 2D extraction from the SEAM model.

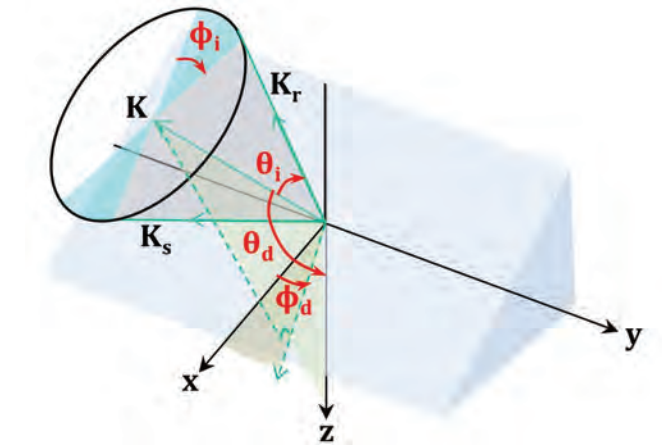

Figure 1. An illustration of incident-azimuth and dip-azimuth angle definition in RTM 3D dip angle gathers for a typical subsurface reflector.

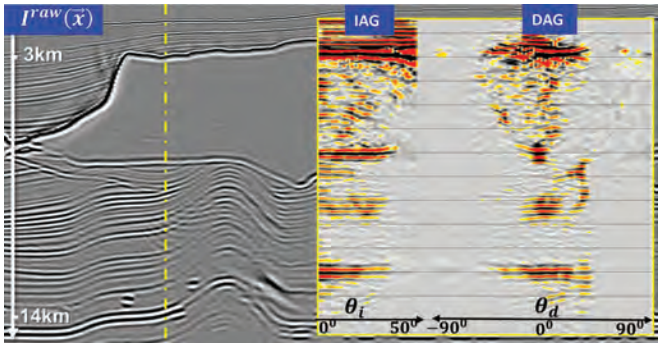

Figure 2. An illustration of RTM incidence and dip angle gather using 2D synthetics.

S/N enhancement using dip gathers

The full, raw RTM stack, $I^{raw}(\vec{x})$, can be obtained from the RTM 3D dip gathers as the straight sum of all the dip contributions, $I^{raw}(\vec{x})=\Sigma_{(\theta_d,\phi_d)}DAG(\vec{x},\theta_d,\phi_d)$. The enhanced RTM 3D dip gathers stack $I^{enh}(\vec{x})$ is obtained by a weighted stack using a scaling matrix, $S(\vec{x},\theta_d,\phi_d;\theta\square,\phi\square)$, that uses a priori dip information ($\theta\square$, $\phi\square$):

$$I^{enh}(\vec{x})=\Sigma_{(\theta_d,\phi_d)}S(\vec{x},\theta_d,\phi_d;\theta\square,\phi\square)DAG(\vec{x},\theta_d,\phi_d). \quad (3)$$

Here, $\vec{x}$ represents the Cartesian coordinates, and $\theta\square$,$\phi\square$, θ_d, ϕ_d are defined specifically for each $\vec{x}$. The scalar function could be of a form such as:

$$S(\vec{x}, \theta_d, \phi_d; \theta\square, \phi\square) = [1 - \sin^2(\theta_d - \theta\square)\sin^2(\phi_d - \phi\square)]^{\alpha(\vec{x})}, \quad (4)$$

where $\alpha(\vec{x})$ is a subjective value based on the level of confidence in the interpretation and the extent of noise contamination. It can be zero for good S/N regions, while a large value may be required to suppress noise in poor S/N regions, especially where the level of confidence in the initial dip information is high because of available dip meters.

For simplicity, we use synthetics generated from the 2D model previously mentioned to demonstrate RTM dip gathers. The red dashed rectangle in Figure 3a indicates an area of steep subsalt bedding contaminated by coherent noise with a flat dip in the RTM straight stack. On the dip gather, strong amplitudes are shown at multiple dip angles, indicating the presence of several dips in the neighborhood of the analysis location. In Figure 3b the fairly flat coherent noise is removed and steeper dip beddings are better revealed by using the proposed weighting scheme. The zoom-in displays in Figures 3c-d are common dip sectors. The spatial dip variations of the signal are effectively preserved and well separated from the noise. The wide dip-angle distribution for fault and point diffractor features is shown in the blue dashed ellipse (Figures 3a-b).

Sensitivity study

Naturally, questions may be raised regarding interpretation-based S/N enhancement, stemming from concerns about the accuracy of the interpretation and the possibility of creating false events from coherent noise. To reinforce our level of confidence in the subsalt image enhanced by RTM 3D dip gathers, we design a sensitivity-analysis procedure using a modified version of the 3D SEAM model with more complex salt to evaluate the impact of interpretation uncertainties.

We selected the three-way closure subsalt area, in which the raw RTM stacked output is noisy (Figure 4a), as the target of our study. We first obtain the true geologic dip from the given reflectivity model and use it as the a priori dip in the RTM dip gather weighted scheme. The resulting image (Figure 4b) has a much more clearly defined structure that matches the structure in the reflectivity model. This indicates the effectiveness of our method. The image is used as a benchmark for the other four tests with different (inaccurate) dip volumes ($\theta\square$, $\phi\square$):

1) true dip scaled by 1/3 (very mild dip, Figure 4c)
2) true dip scaled by 2/3 (slightly less mild dip, Figure 4d)
3) true dip scaled by 4/3 (slightly steeper dip, Figure 4e)
4) an orthogonal dip field (Figure 4f)

Furthermore, similarity cubes are generated by computing cross-correlations along the different dip fields. The higher coherency values indicate a higher S/N, while lower values indicate a lower S/N.

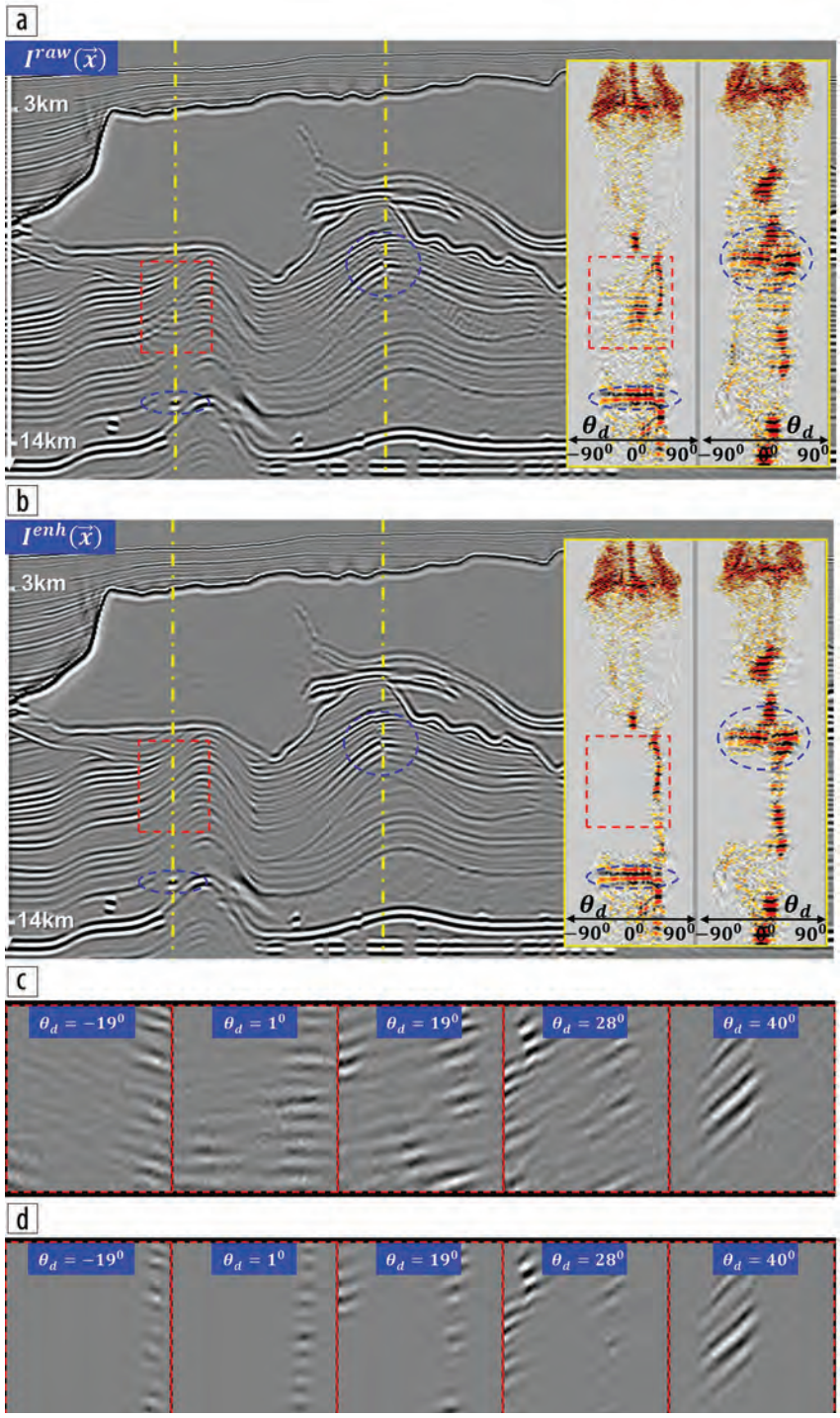

Figure 3. RTM 3D dip gather enhancement in a 2D model. (a) Straight-stack RTM output and corresponding raw dip gathers from the locations indicated by yellow lines. (b) Dip gather enhanced stack and corresponding scaled dip gathers. (c) Zoom-in of the raw common dip/azimuth sector ($\theta_d = -19^0, 1^0, 19^0, 28^0, 40^0$; $\phi_d = 0^0$) indicated by the red dashed rectangle. (d) Zoom-in of the same scaled common dip/azimuth sector.

Comparing the enhanced images (Figures 4b-4f) to the raw stack (Figure 4a) and coherency histogram, we make the following observations:

- A completely geologically implausible dip field results in a noncoherent image. Structure continuities from good S/N zones are lost (Figure 4f).
- The structure coherency decreases with increasing dip error. The larger the dip error, the worse the structure discontinuities become.
- Migration noise, rather than true events, can be enhanced when using incorrect a priori dip fields, resulting in less focused and less coherent structures (Figure 4c).
- Small dip errors may generate visually acceptable structure continuities. However, the coherency along the guided dip field is still poor (Figure 4e).
- True geologic dip fields generate the best enhanced volume with realistic seismic characteristics and fewer contradicting dips.

The above observations suggest that the coherent structures obtained from stacking the weighted RTM 3D dip gathers are trustworthy if the interpretations are correct. They also demonstrate the potential for evaluating interpretation accuracy by visually comparing the 3D seismic character of interpretation-based dip RTM enhancement volumes with the raw RTM. An extension of this method is to conduct subsalt interpretation scenario studies to tackle interpretation uncertainties in poor illumination regions. Since weightings are applied postmigration and there is no modeling work involved, the cost will not increase significantly, even when evaluating a large number of different interpretation scenarios.

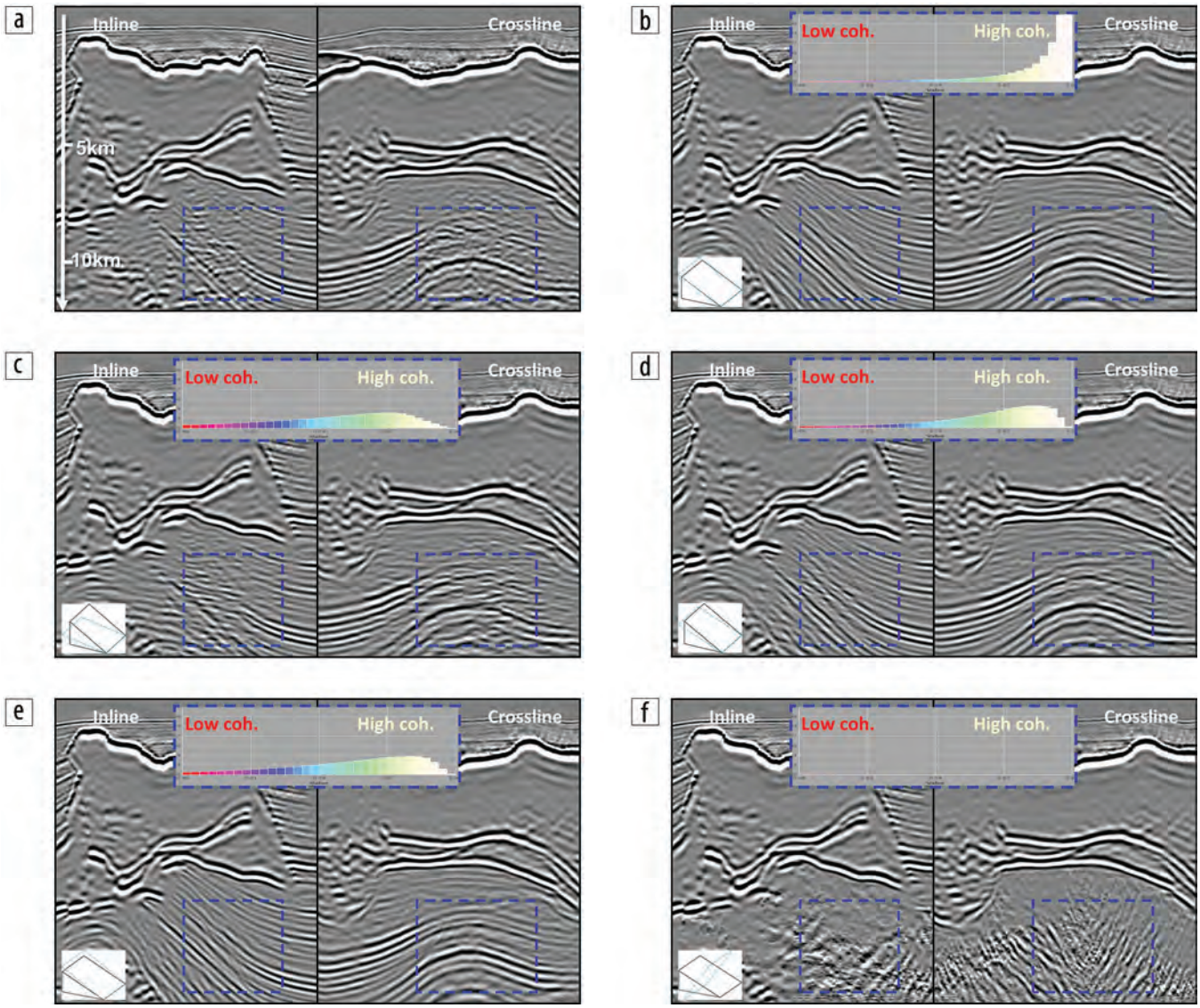

Figure 4. Sensitivity study of the modified 3D SEAM model. (a) RTM straight-stack output. Dip gather enhanced stack with structure-oriented correlation cube overlaid from (b) true geologic dip, (c) a much milder dip, (d) a slightly milder dip, (e) a slightly steeper dip, and (f) an orthogonal dip. The insets are histograms of coherency values for each scenario from the target area (indicated by the blue dashed rectangles).

Real data example with a staggered-acquisition FAZ survey

We apply interpretation-guided RTM dip gather enhancement to a real data set from a staggered-acquisition FAZ survey acquired in the Keathley Canyon area of the GoM. The acquisition configuration provided FAZ (up to 10 km), ultralong offsets (up to 18 km), and broad bandwidth due to variable-depth streamer towing (Mandroux et al., 2013). The imaging challenge for this test region is an anticline with steeply dipping sides; the area suffers from poor illumination due to the discordant dip of the overlying base of salt.

To evaluate the contribution of additional data acquired with this acquisition configuration compared to wide azimuth (WAZ), we select a subset of the FAZ acquisition to simulate a WAZ acquisition and compare the corresponding image to the complete FAZ data. The comparison of the two RTM straight stack results is inconclusive; no obvious image improvements were observed from the simple inclusion of far offsets and more azimuths (Figures 5a and 5c). Actually, in both cases the noise overwhelms the stack image, while the energy contributing to the true dips is suppressed.

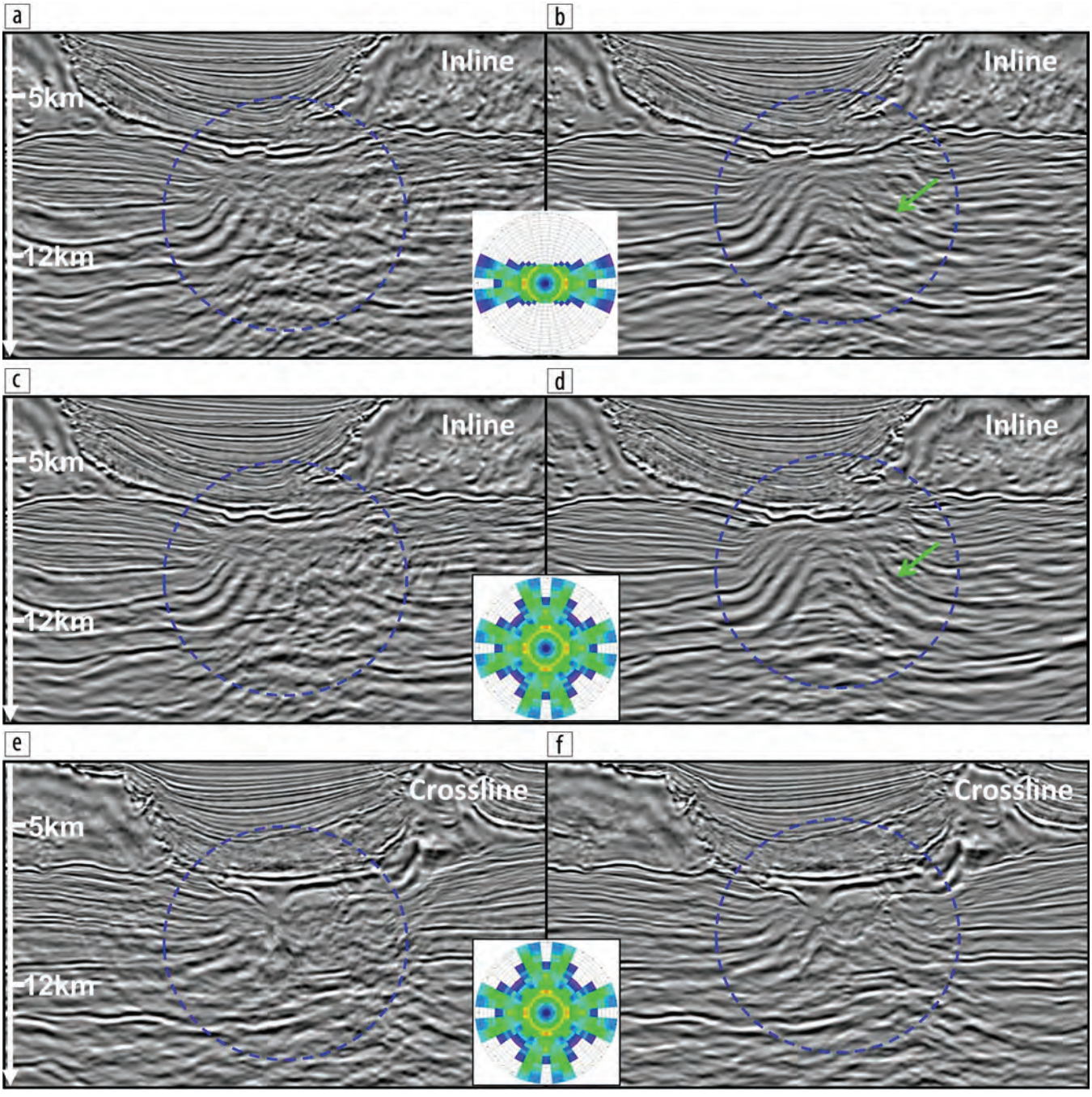

Figure 5. Dip gather enhancement of Gulf of Mexico full-azimuth data. (a) Straight-stack RTM with wide-azimuth (WAZ) data selection. (b) Dip gather enhanced stack with WAZ data selection. (c) Straight stack RTM with full-azimuth data. (d) Dip gather enhanced stack with full-azimuth data. (e) Corresponding crossline view of (c). (f) Corresponding crossline view of (d). Overlaid rose (offset azimuth) diagrams illustrate the data selection for the stack images.

To reveal the true recorded-signal contribution, we use RTM 3D dip gathers along with interpretation to separate the dipping events identified as noise. Figures 5b and 5d show that RTM 3D dip gather weighting enhances the previously noisy zone of the migrated section (circled in blue) compared to the raw stacks (Figures 5a and 5c, respectively). More interestingly, compared to the WAZ data (Figure 5b), the hidden steep dips beneath the right side of the salt body are revealed with the FAZ data (Figure 5d). This suggests that long offsets and/or full-azimuth surface seismic data are required to image these complex subsalt structures, but they still demand additional effort to separate the signal. To further demonstrate the improvement on the whole anticline structure, corresponding crossline images are shown in Figures 5e and 5f.

Discussion and conclusions

The proposed interpretation-guided weighting scheme on RTM 3D dip gathers can effectively attenuate coherent noise on the synthetic and real data tests. FAZ acquisition configurations generally provide better illumination of the subsurface. However, the upgrading of acquisition techniques does not necessarily eliminate the merit of S/N-enhancing techniques for better subsalt imaging. Although the computational cost of generating RTM 3D dip gathers can be high, the increase in S/N resulting from educated weighting and the ability to quickly evaluate several different interpretation scenarios justify the cost.

Sensitivity tests provide some insight on the impact of inaccurate initial dipping interpretations and indicate that a more accurate interpretation can lead to a better signal enhancement. As an additional benefit, a sensitivity analysis may be utilized for detecting incorrect interpretations in a quantitative way. TLE

Acknowledgments

We thank CGG for permission to publish these results and Tony Huang and Yunfeng Li for constructive feedback and discussion. We also thank the SEG Advanced Modeling (SEAM) project for providing the synthetic model used in this paper.

Corresponding author: Yi.Huang@CGG.com

References

Chazalnoel, N., B. Ong, and W. Zhao, 2012, Imaging 3-way closures by combining a deconvolution imaging condition with vector offset output RTM: 82nd Annual International Meeting, SEG, Expanded Abstracts, http://dx.doi.org/10.1190/segam2012-1271.1.

Fletcher, P. R., S. Archer, D. Nichols, and W. Mao, 2012, Inversion after depth imaging: 82nd Annual International Meeting, SEG, Expanded Abstracts, http://dx.doi.org/10.1190/segam2012-0427.1.

Gherasim, M., U. Albertin, B. Nolte, O. J. Askim, M. Trout, and K. Hartman, 2010, Wave-equation angle-based illumination weighting for optimized subsalt imaging: 80th Annual International Meeting, Expanded Abstracts, 3293–3297, http://dx.doi.org/10.1190/1.3513532.

Huang, Y., W. Gou, O. Leblanc, L. Yang, S. Ji, and Y. Huang, 2013, Study and application of salt-related converted waves in imaging: 83rd Annual International Meeting, SEG, Expanded Abstracts, 3851–3855, http://dx.doi.org/10.1190/segam2013-1291.1.

Li, Z., B. Tang, and S. Ji, 2012, Subsalt illumination analysis using RTM 3D dip gathers: 82nd Annual International Meeting, SEG, Expanded Abstracts, http://dx.doi.org/10.1190/segam2012-1348.1.

Mandroux, F., B. Ong, C. Ting, S. Mothi, T. Huang, and Y. Li, 2013, Broadband, long-offset, full-azimuth, staggered marine acquisition in the Gulf of Mexico: First Break, **31**, 125–132.

Nemeth, T., C. Wu, and G. T. Schuster, 1999, Least-square migration of incomplete reflection data: Geophysics, **64**, no. 1, 208–221, http://dx.doi.org/10.1190/1.1444517.

Ting, C., L. Zhuo, and Z. Yuan, 2010, Quest for subsalt steep dips: Presented at the SEG/EAGE Summer Research Workshop, 2010.

Xu, Q., Y. Li, X. Yu, and Y. Huang, 2011, Reverse time migration using vector offset output to improve sub-salt imaging — A case study at the Walker Ridge GOM: 81st Annual International Meeting, SEG, Expanded Abstracts, 3269–3274, http://dx.doi.org/10.1190/1.3627875.

Xu, S., Y. Zhang, and B. Tang, 2011, 3D angle gathers from reverse time migration: Geophysics, **76**, no. 2, S77–S92, http://dx.doi.org/10.1190/1.3536527.